# Supporting Information

# Design and Mechanism of Tetrahydrothiophene-based GABA-Aminotransferase Inactivators

Hoang V. Le,[1] Dustin D. Hawker,[1] Rui Wu,[2] Emma Doud,[3] Julia Widom,[1] Ruslan Sanishvili,[4] Dali Liu,[2] Neil L. Kelleher,[3] Richard B. Silverman*,[1]

[1] Departments of Chemistry and Molecular Biosciences, Chemistry of Life Processes Institute, and the Center for Molecular Innovation and Drug Discovery, Northwestern University, Evanston, IL 60208

[2] Department of Chemistry and Biochemistry, Loyola University Chicago, Chicago, IL 60660

[3] Departments of Chemistry and Molecular Biosciences, and the Proteomics Center of Excellence, Northwestern University, Evanston, IL 60208

[4] X-ray Science Division, Advanced Photon Source, Argonne National Laboratory, Lemont, IL 60439

**Table S1.** Crystallographic Data Collection and Refinement Statistics

| Data set | Inactivated GABA-AT |
|---|---|
| PDB code | 4YoI |
| Space Group | $P2_1$ |
| Cell Dimensions | |
| a (Å) | 69.5 |
| b (Å) | 226.8 |
| c (Å) | 71.4 |
| α = γ (°) | 90 |
| B (°) | 108.8 |
| Resolution (Å) | 36.07-1.66 |
| [a]$R_{merge}$ (%) | 5.7 (66.4) |
| I/sigma | 12.5 (1.0) |
| Completeness (%) | 97.0 (94.0) |
| Redundancy | 3.8 (3.6) |
| No. Total reflections | 892525 |
| No. Unique reflections | 236557 |
| [b]$R_{work}$ / [c]$R_{free}$ (%) | 17.2/20.4 |
| No. of Atoms | 17167 |
| No. of Solvent Atoms | 2239 |
| B-factors (Å$^2$) | |
| Overall | 22.9 |
| Ligand | 9.53 / 28.86 |
| [d]RMSD Bond Length (Å) | 0.007 |
| [d]RMSD Bond Angles (°) | 1.105 |
| Ramachandran | |
| Favored (%) | 95.8 |
| Allowed (%) | 3.90 |
| Outlier (%) | 0.30 |

The values for the highest resolution bin are in parentheses.

[a]Linear $R_{merge} = \Sigma|I_{obs}-I_{avg}|/ \Sigma I_{avg}$

[b]$R_{cryst} = \Sigma|F_{obs}-F_{calc}|/ \Sigma F_{obs}$.

[c]Five percent of the reflection data were selected at random as a test set and only these data were used to calculate $R_{free}$.

[d]RMSD, root mean square deviation.

ND, Not Determined/Calculated by the program

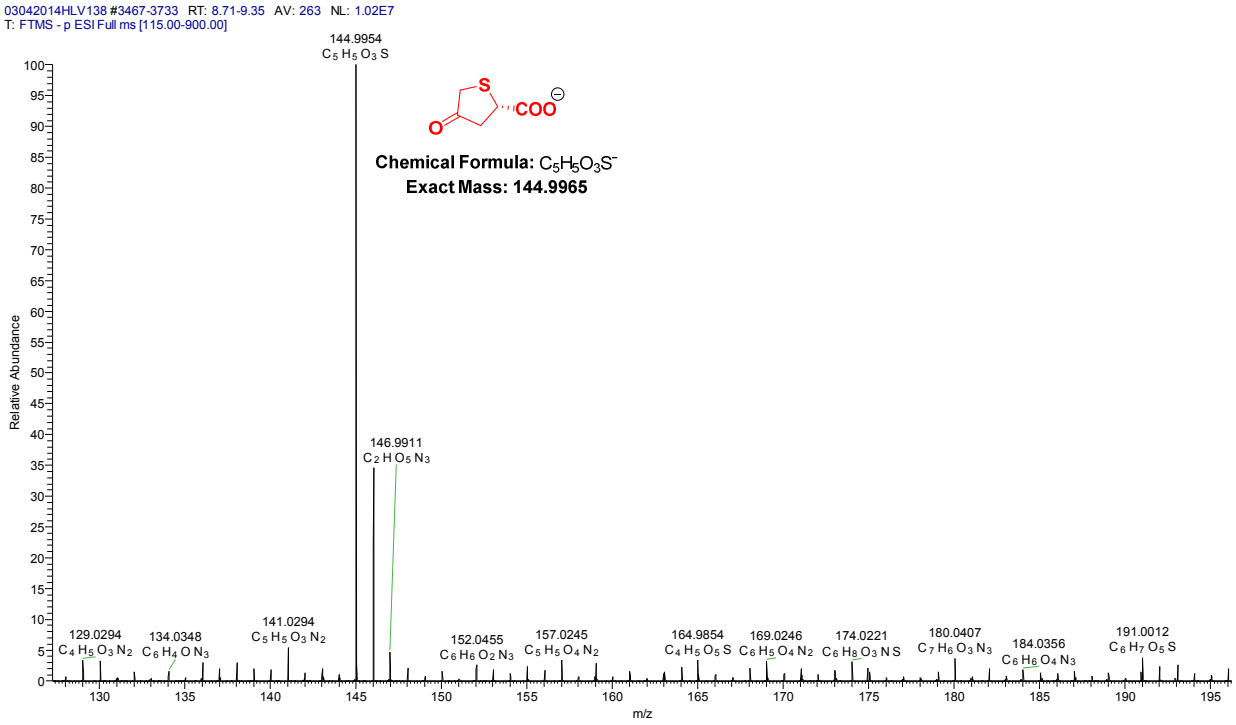


**Figure S1.** High-Resolution Mass Spectrum of Metabolite **36**

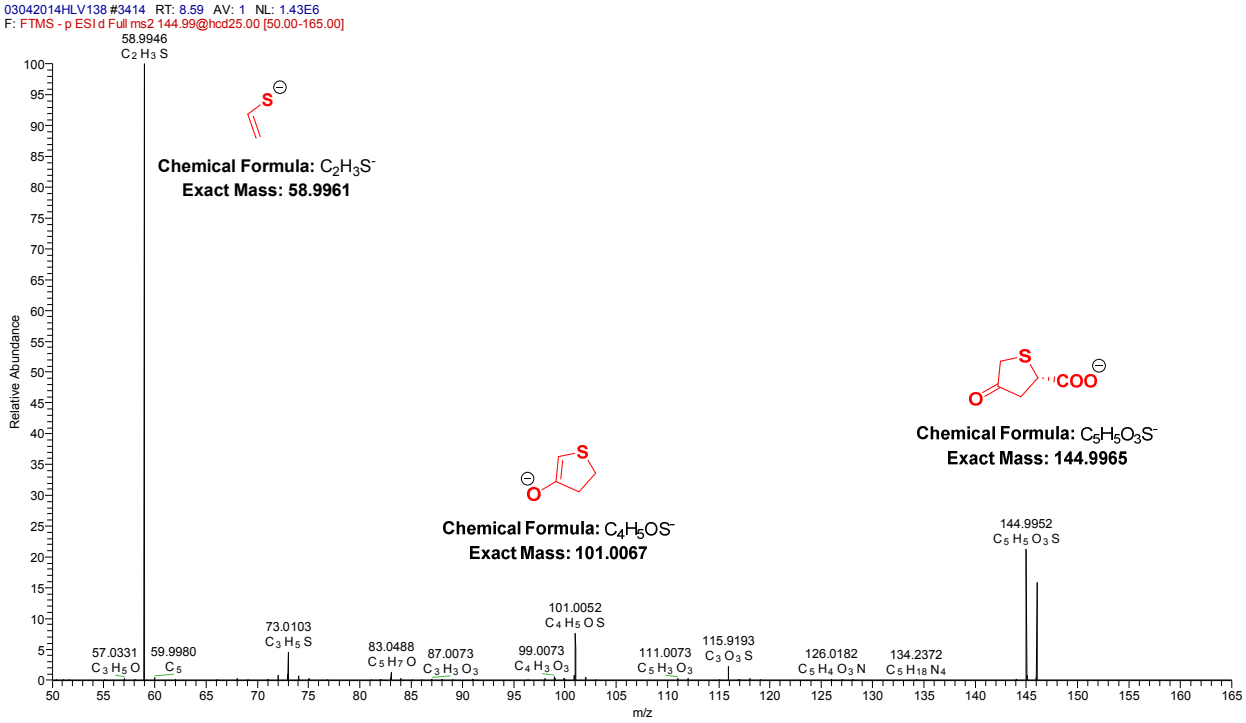


**Figure S2.** Fragmentation and Assigned Structures of *m/z* 144.9954

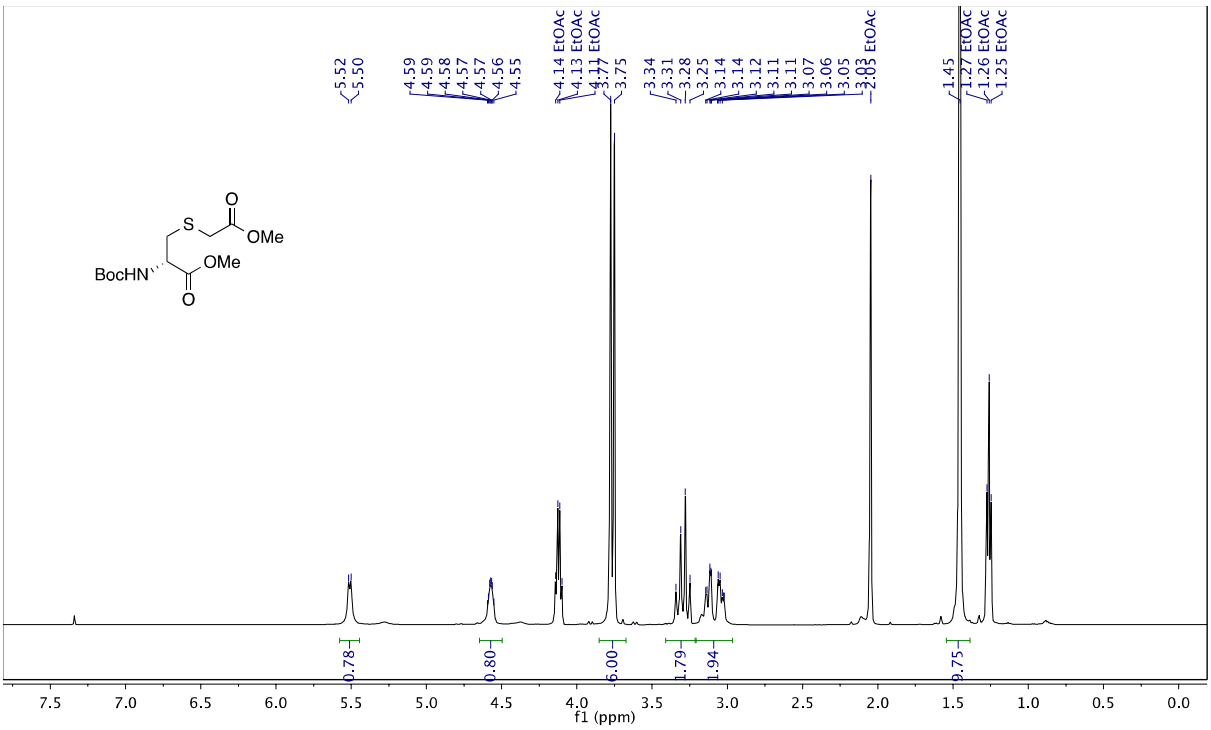


**Figure S3.** $^{1}$H NMR Spectrum of **24**

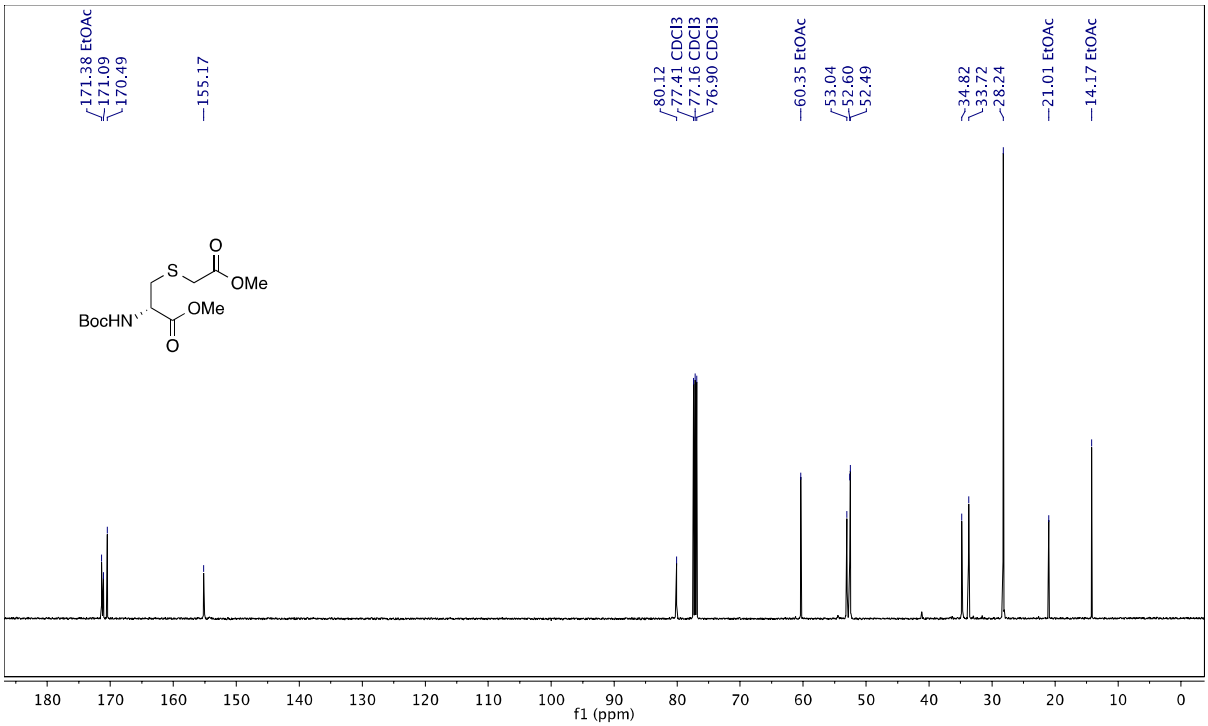


**Figure S4.** $^{13}$C NMR Spectrum of **24**

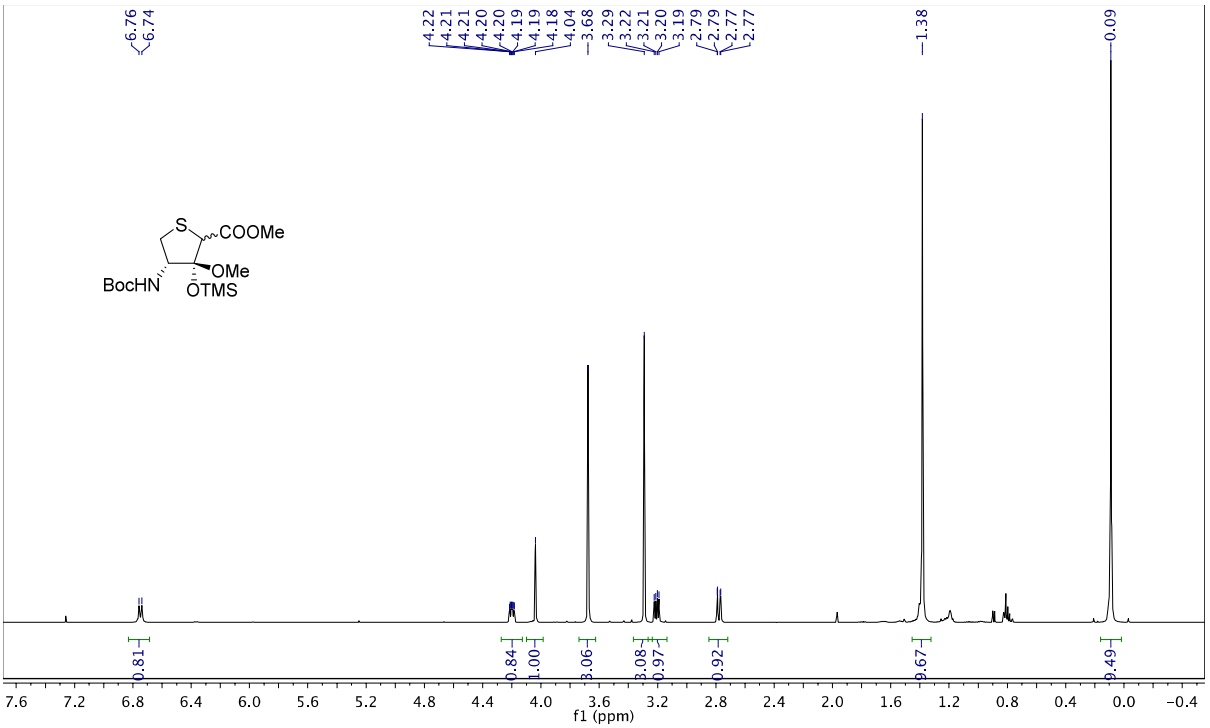


**Figure S5.** [1]H NMR Spectrum of **26**

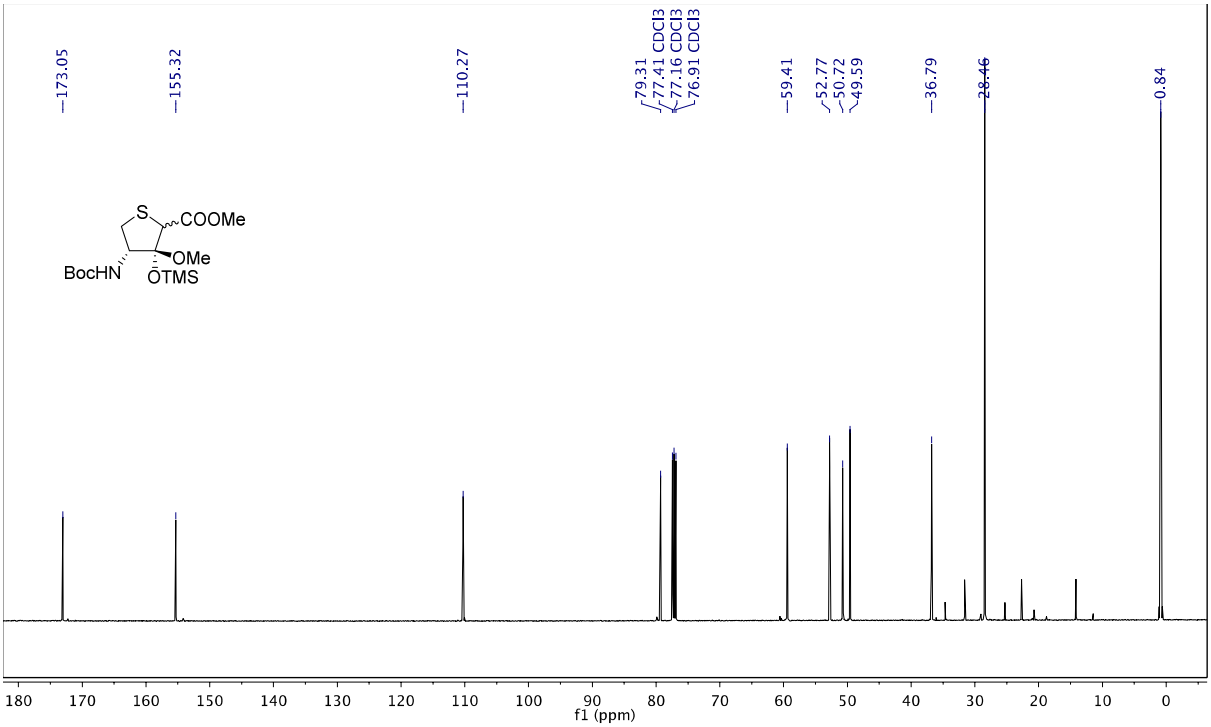


**Figure S6.** [13]C NMR Spectrum of **26**

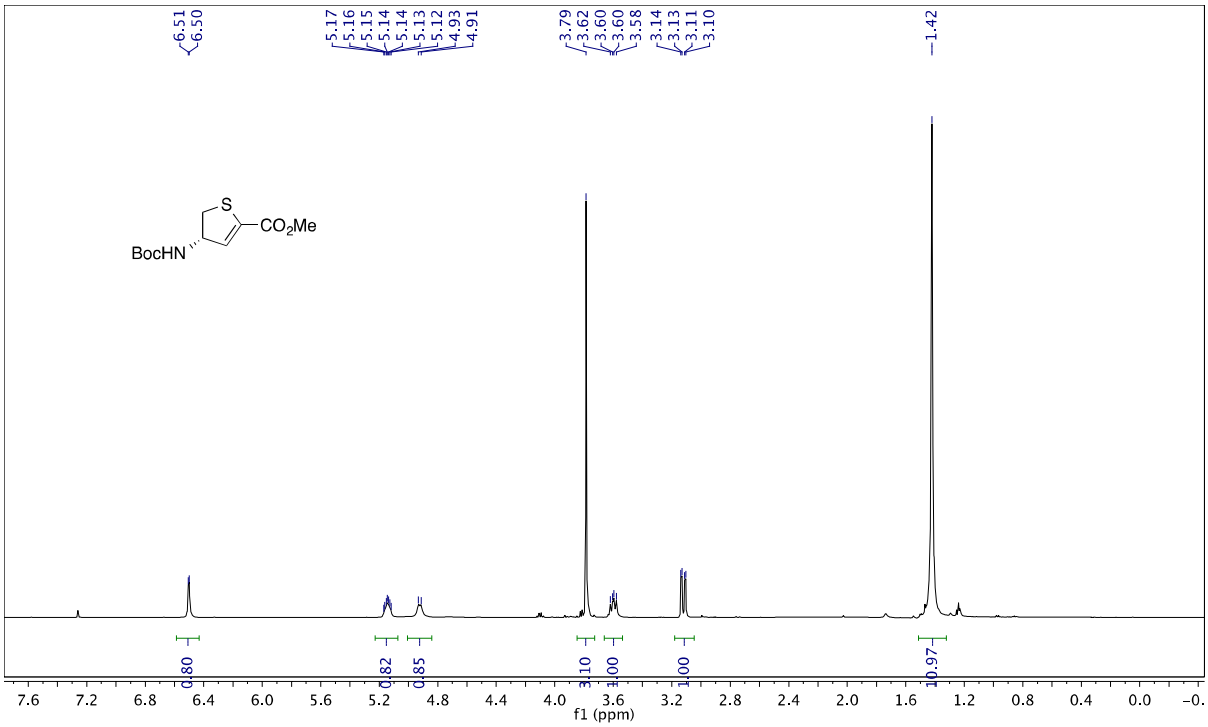


**Figure S7.** $^{1}$H NMR Spectrum of **28**

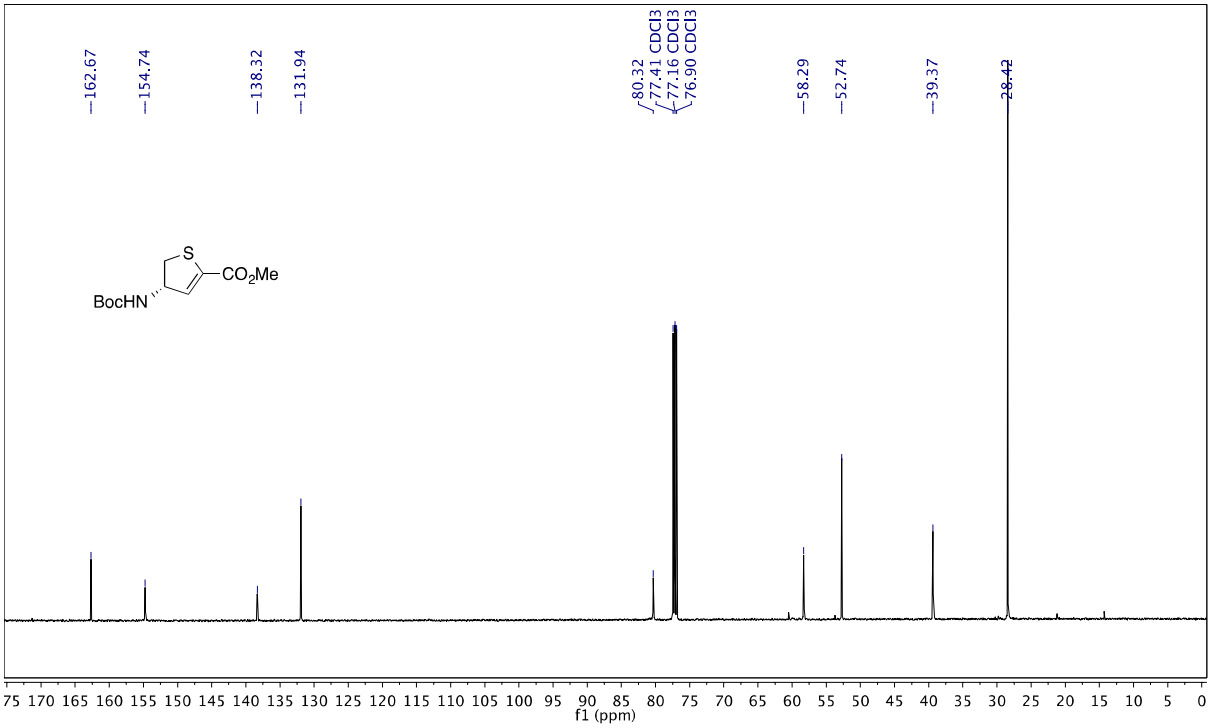


**Figure S8.** $^{13}$C NMR Spectrum of **28**

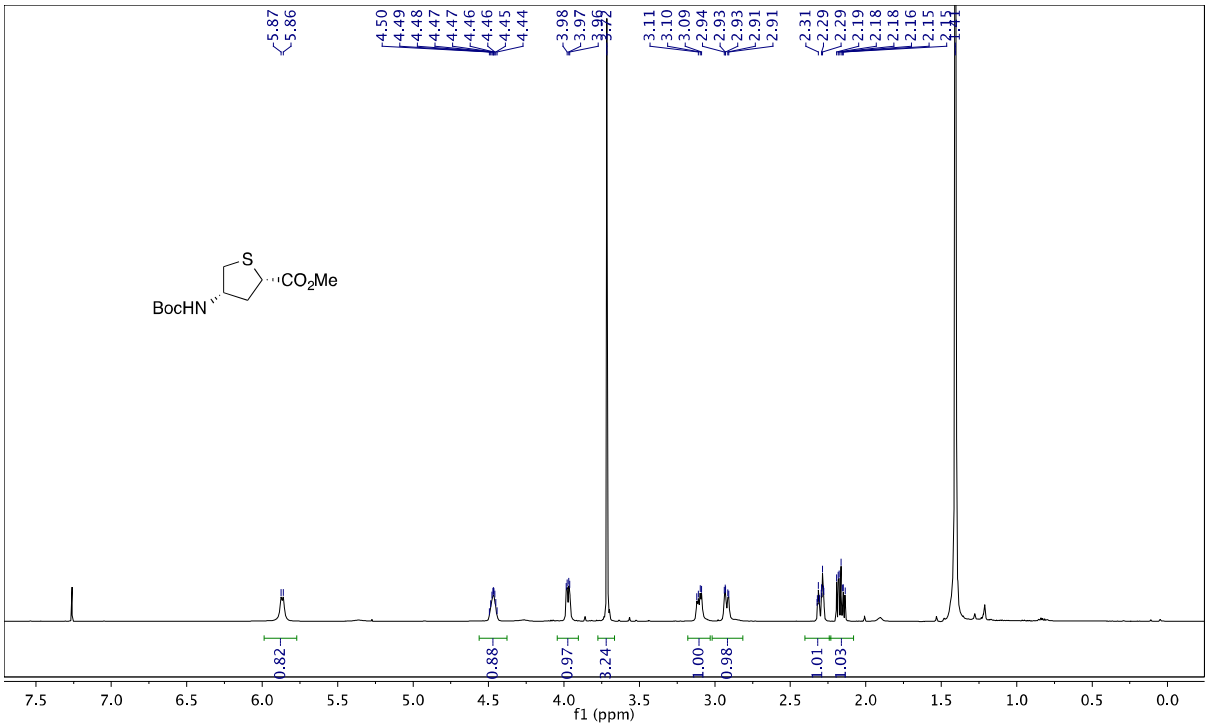


**Figure S9.** [1]H NMR Spectrum of **29**

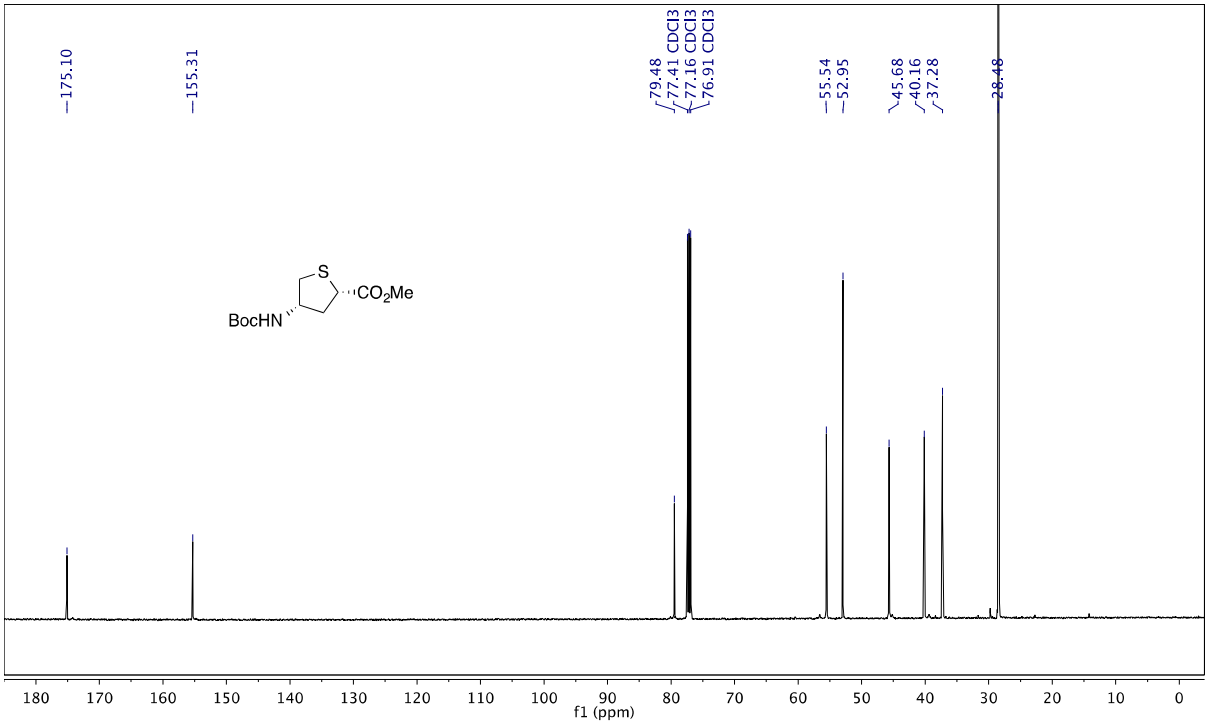


**Figure S10.** [13]C NMR Spectrum of **29**

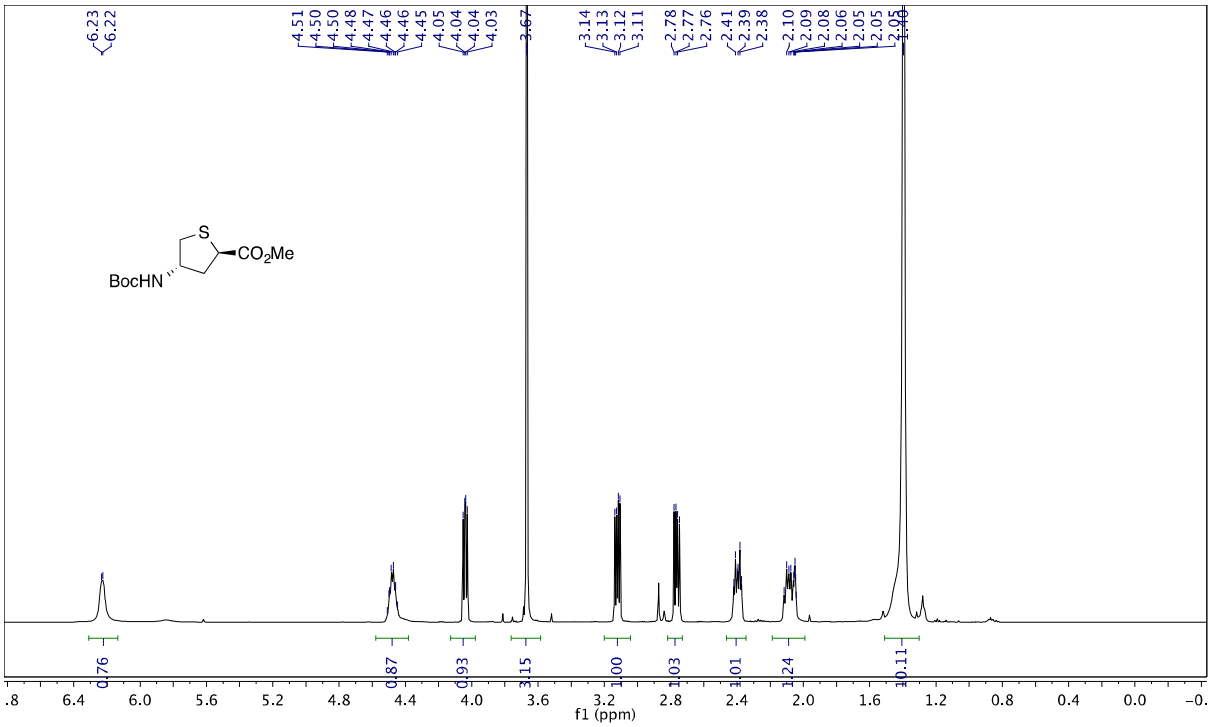


**Figure S11.** $^{1}$H NMR Spectrum of **30**

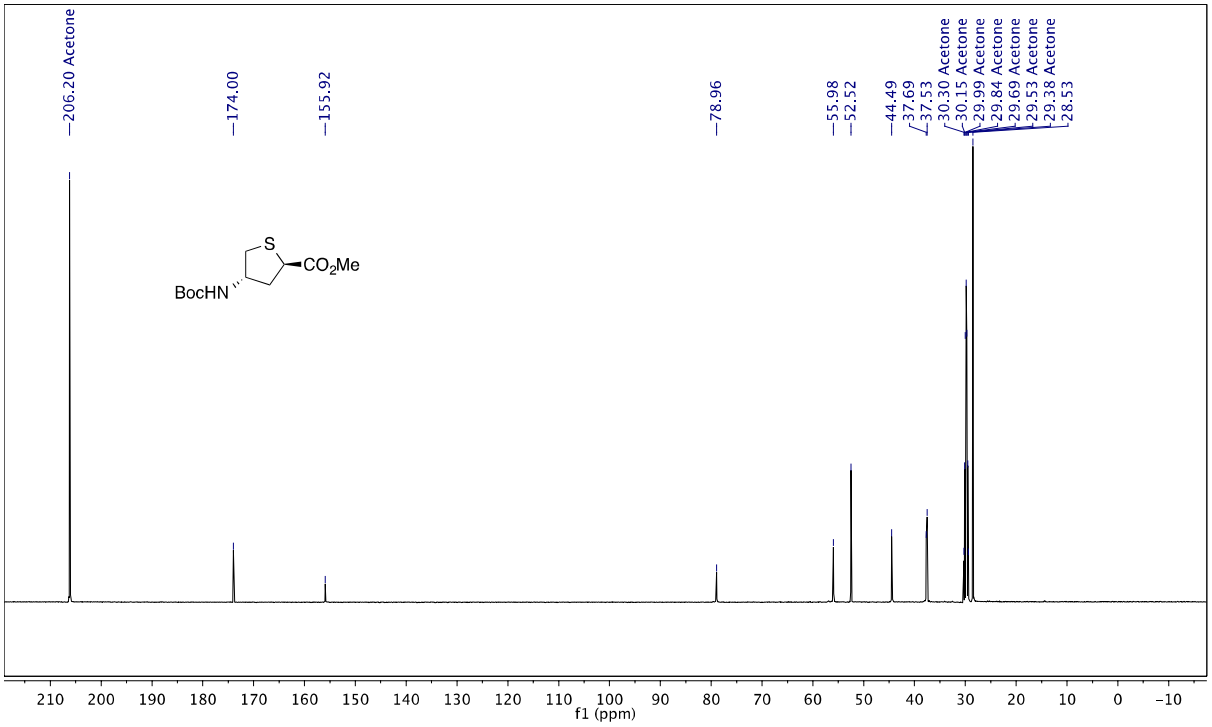


**Figure S12.** $^{13}$C NMR Spectrum of **30**

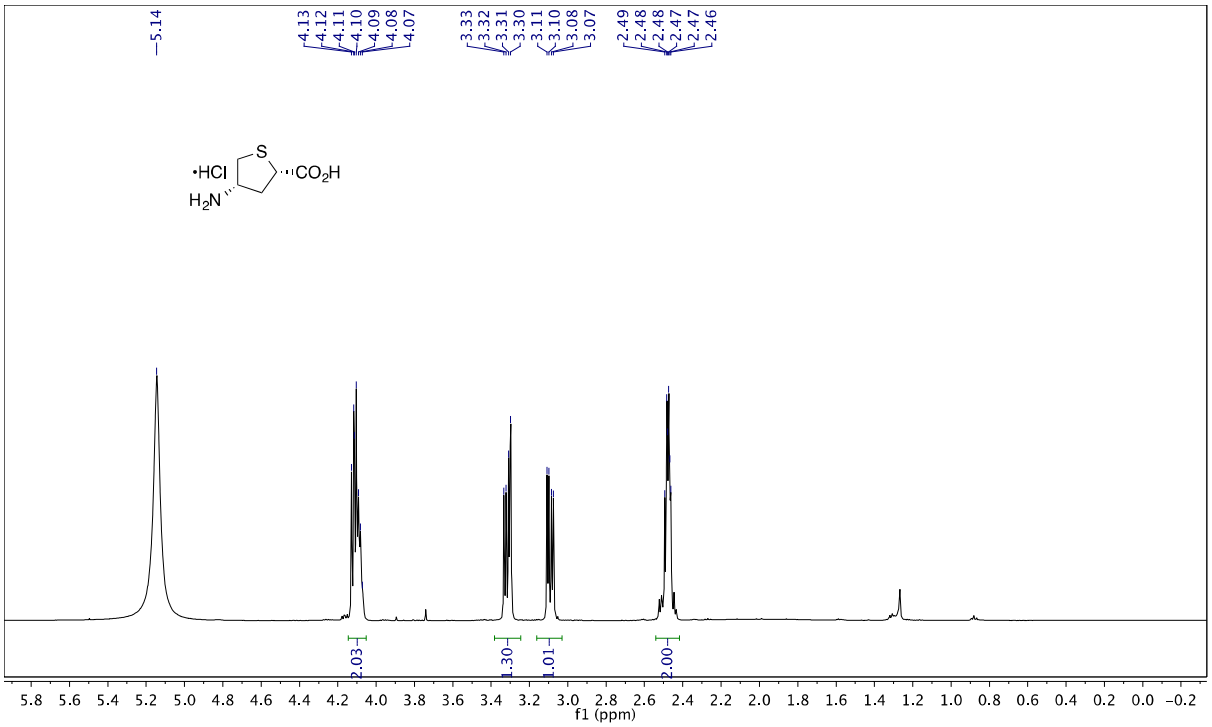


**Figure S13.** $^{1}$H NMR Spectrum of **17**

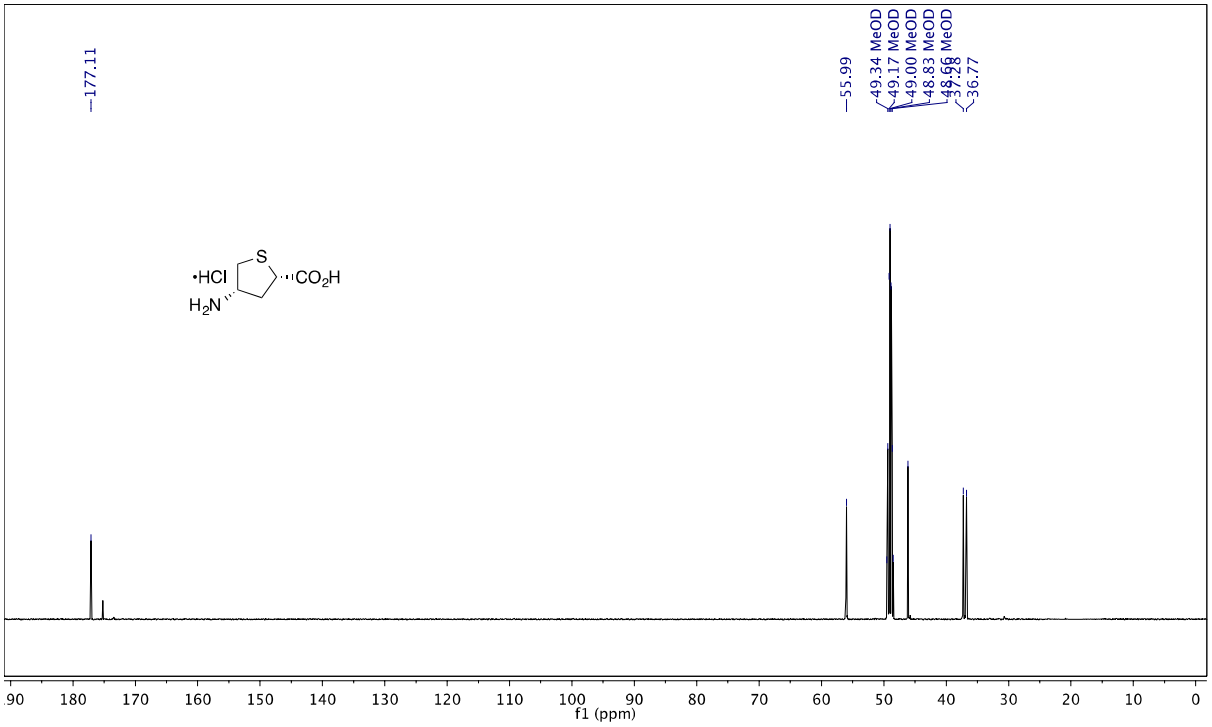


**Figure S14.** $^{13}$C NMR Spectrum of **17**

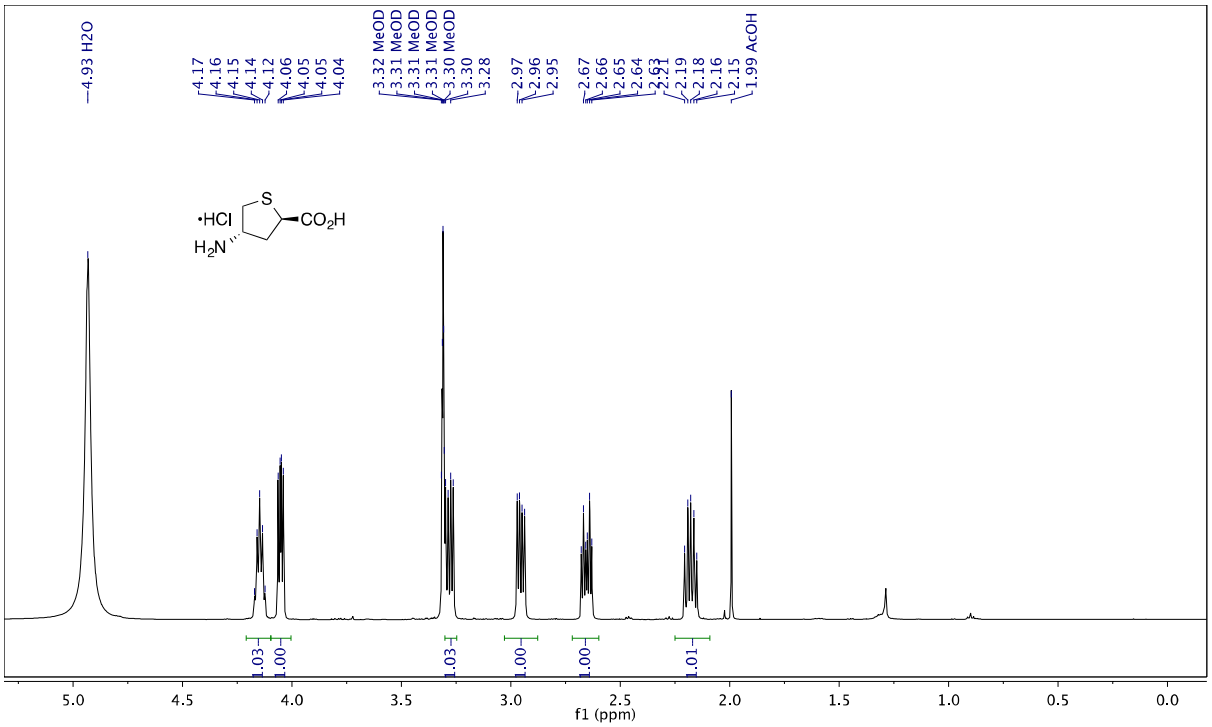


**Figure S15.** $^{1}$H NMR Spectrum of **18**

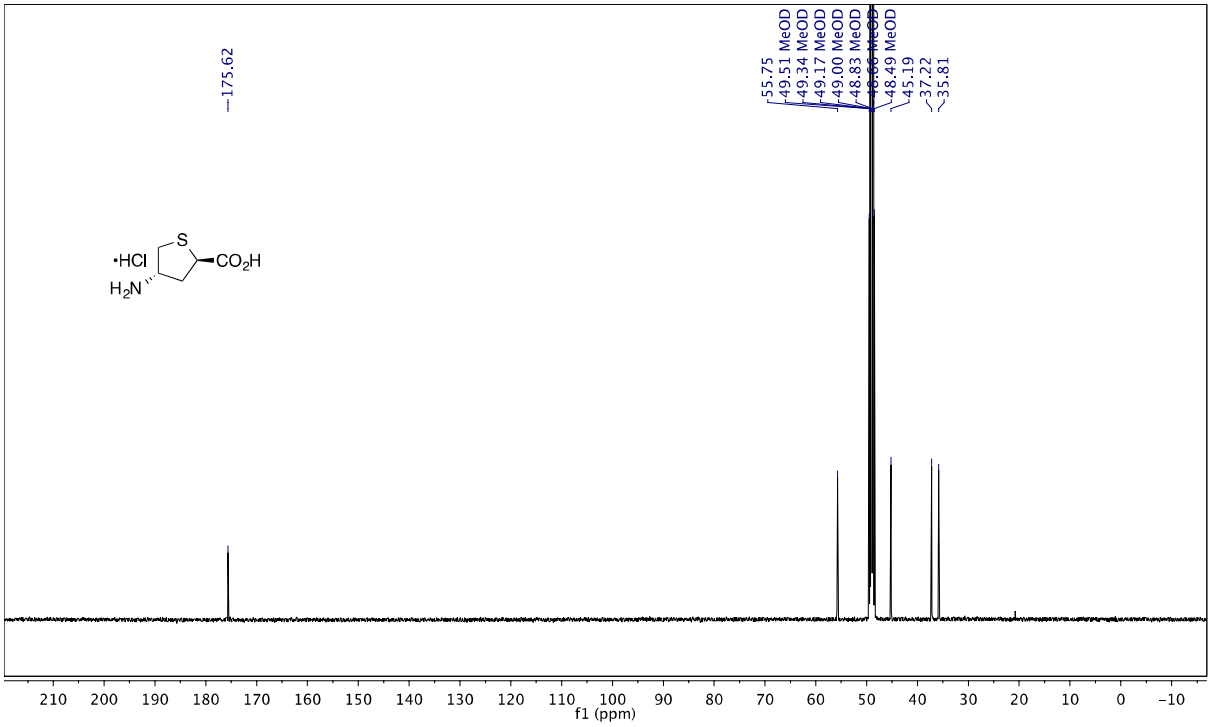


**Figure S16.** $^{13}$C NMR Spectrum of **18**

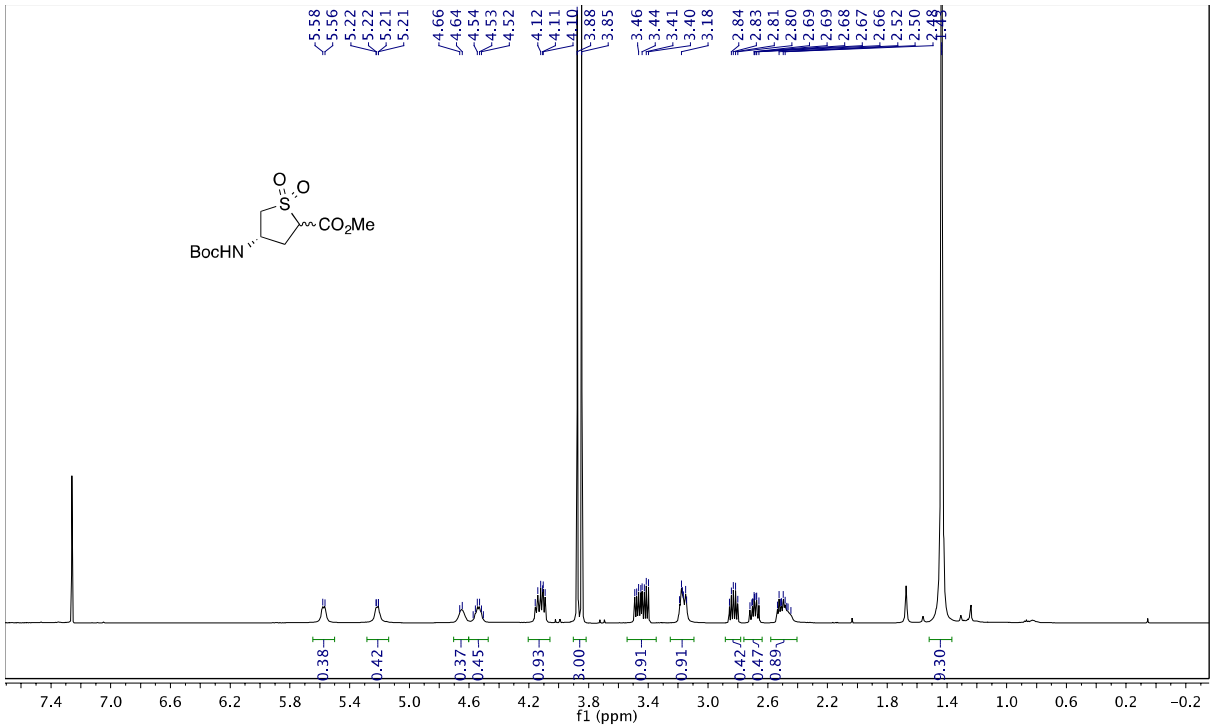


**Figure S17.** [1]H NMR Spectrum of **31**

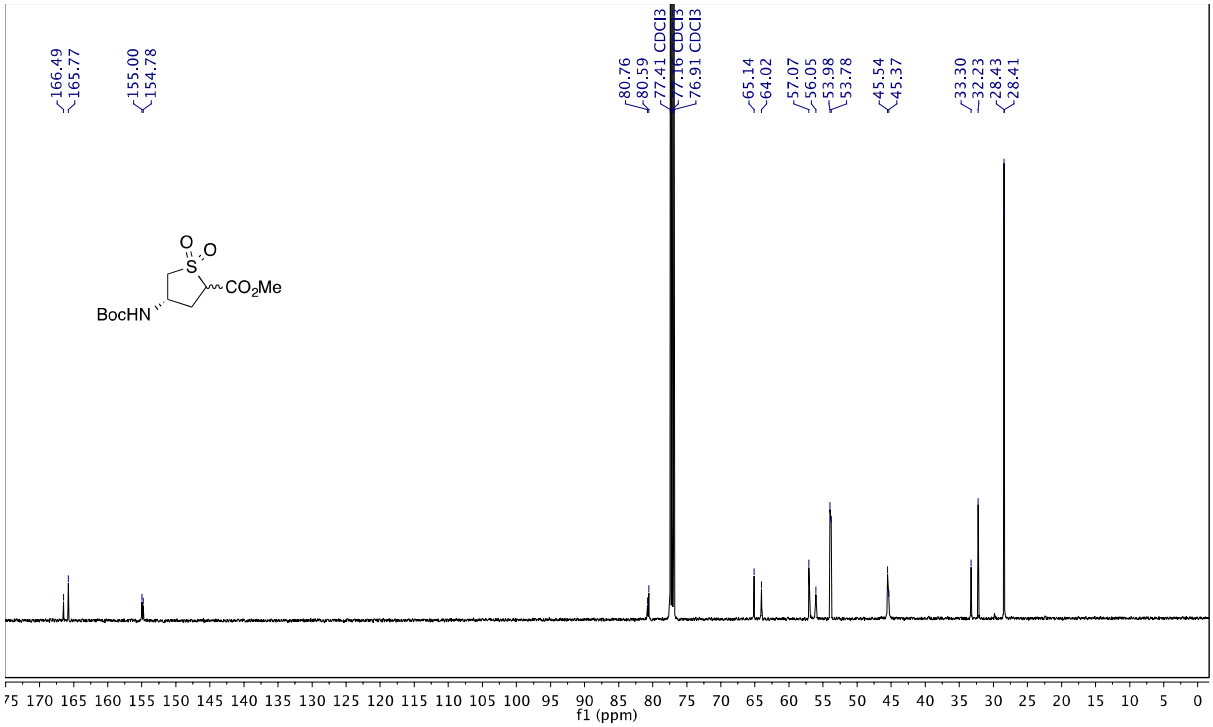


**Figure S18.** [13]C NMR Spectrum of **31**

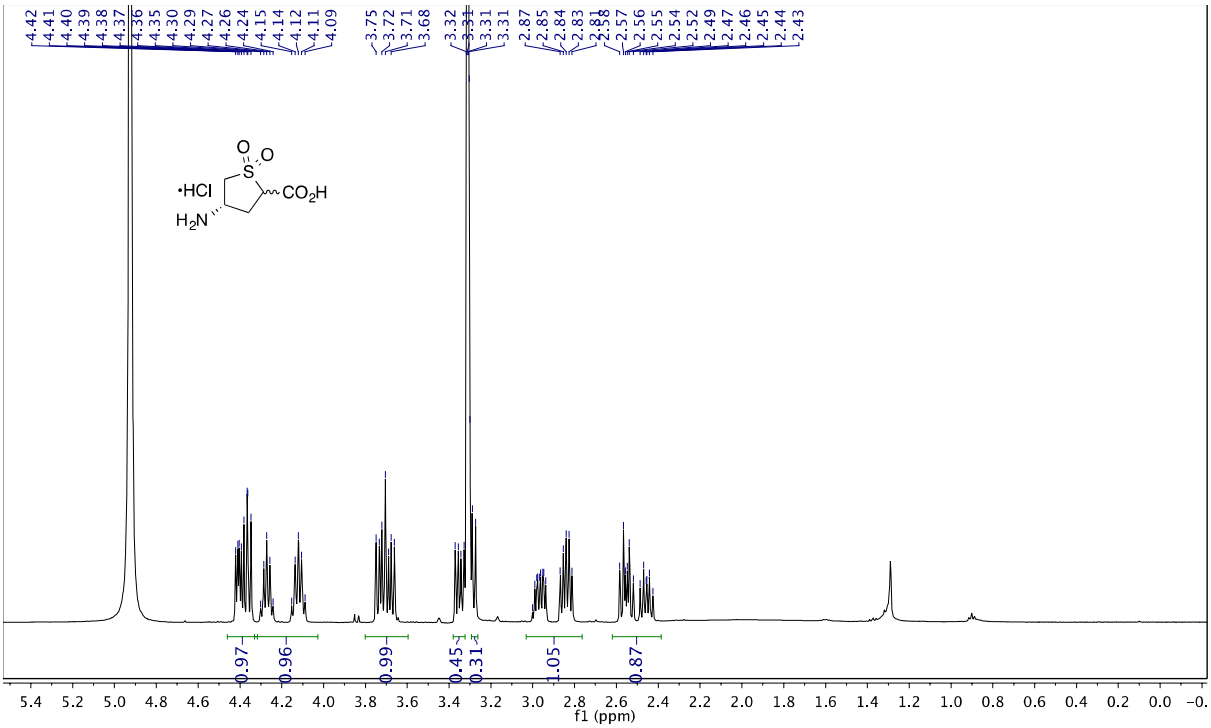


**Figure S19.** $^{1}$H NMR Spectrum of **19**

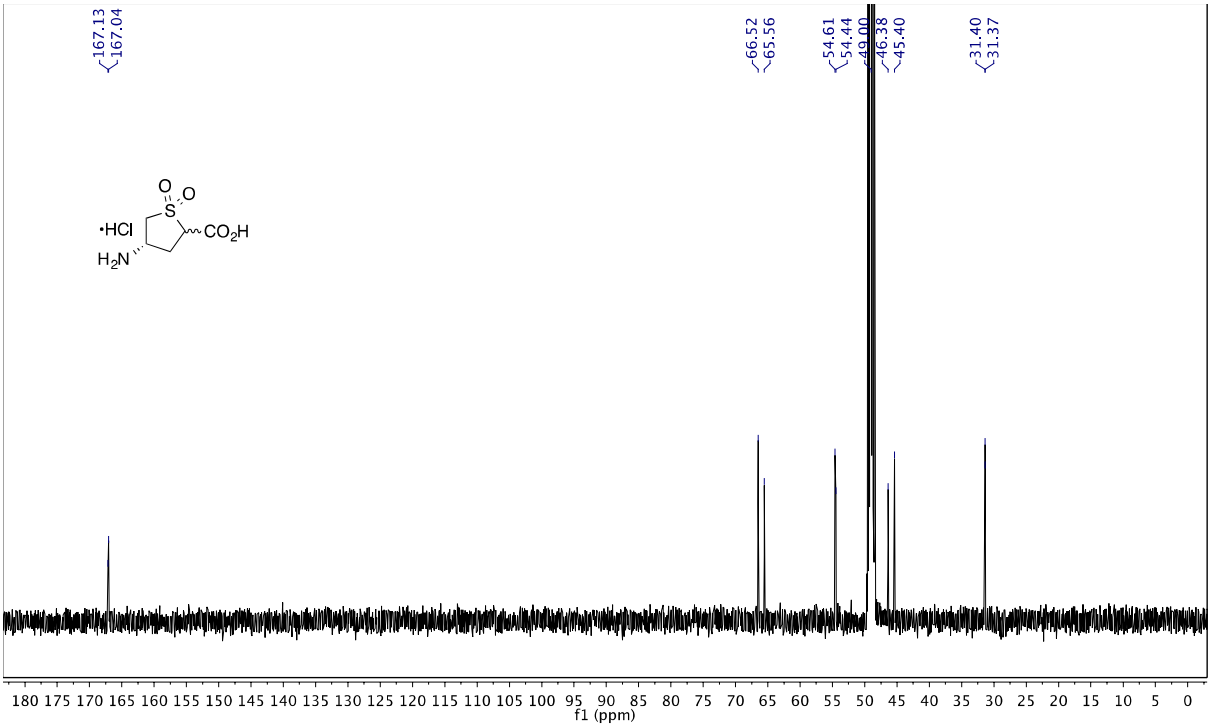


**Figure S20.** $^{13}$C NMR Spectrum of **19**

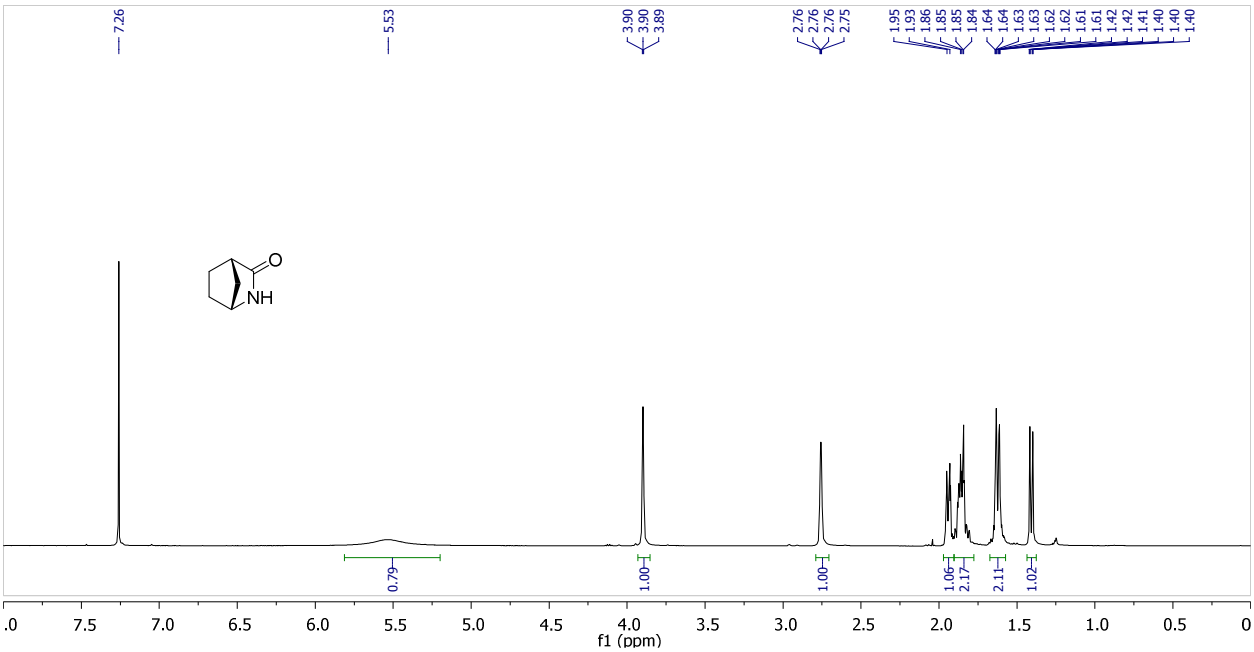


**Figure S21.** $^{1}$H NMR Spectrum of **38**

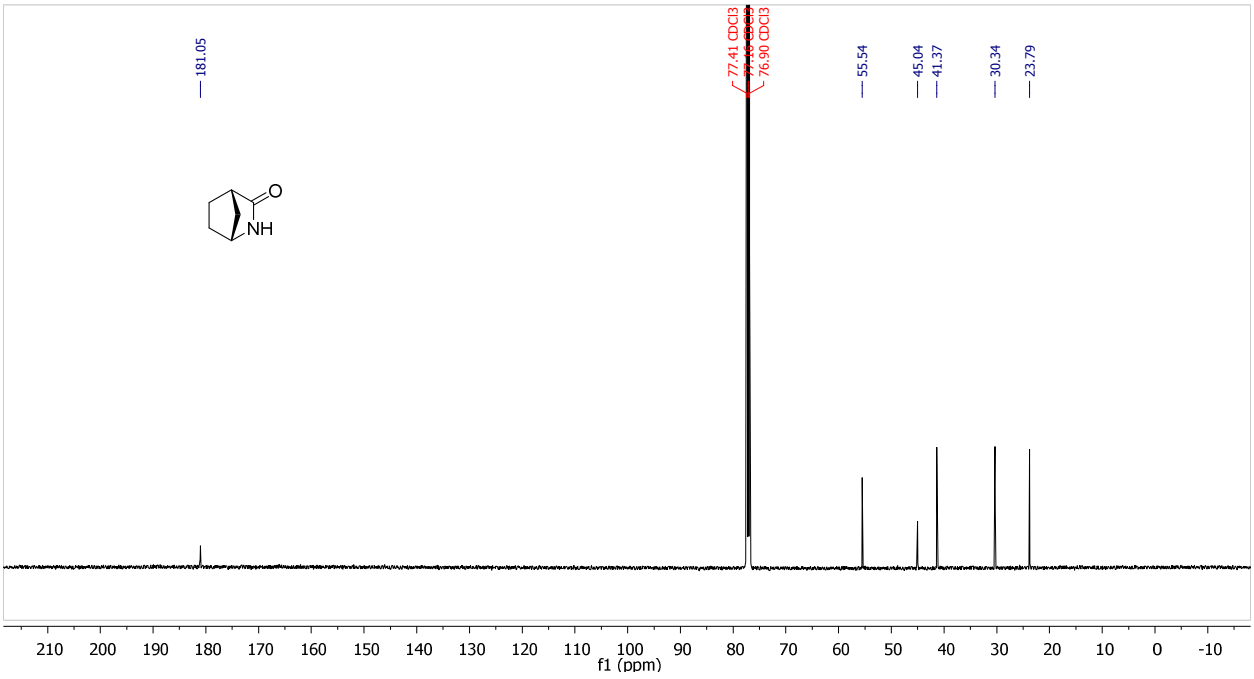


**Figure S22.** $^{13}$C NMR Spectrum of **38**

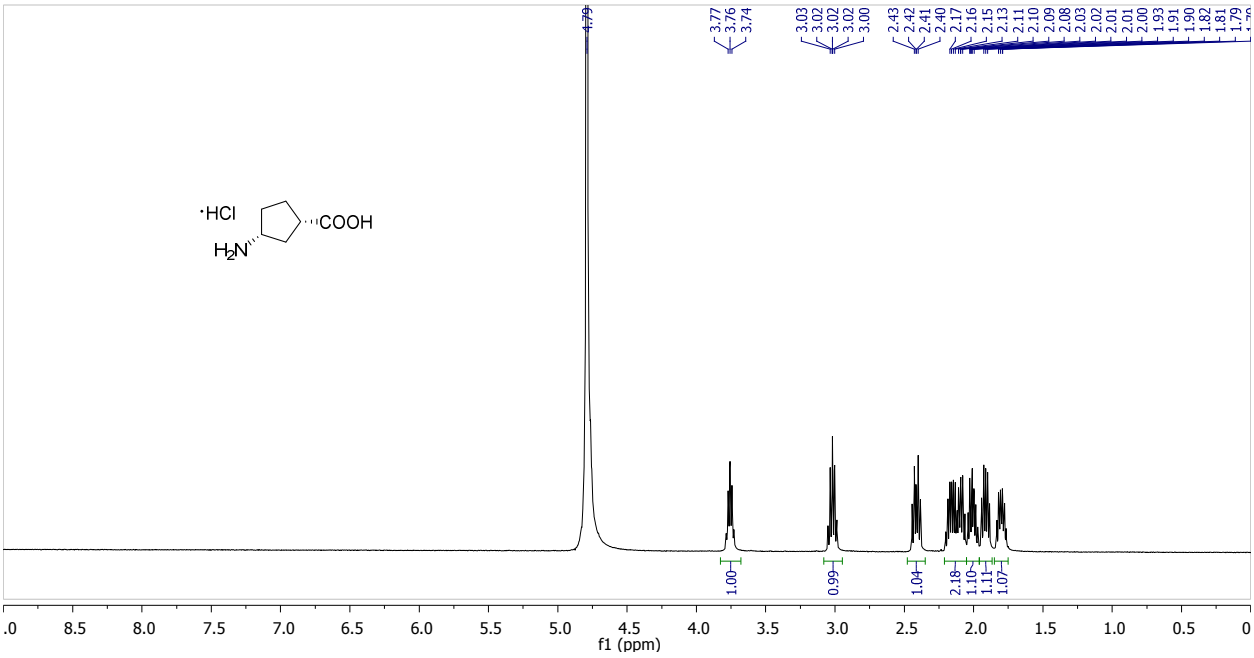


**Figure S23.** [1]H NMR Spectrum of **39**

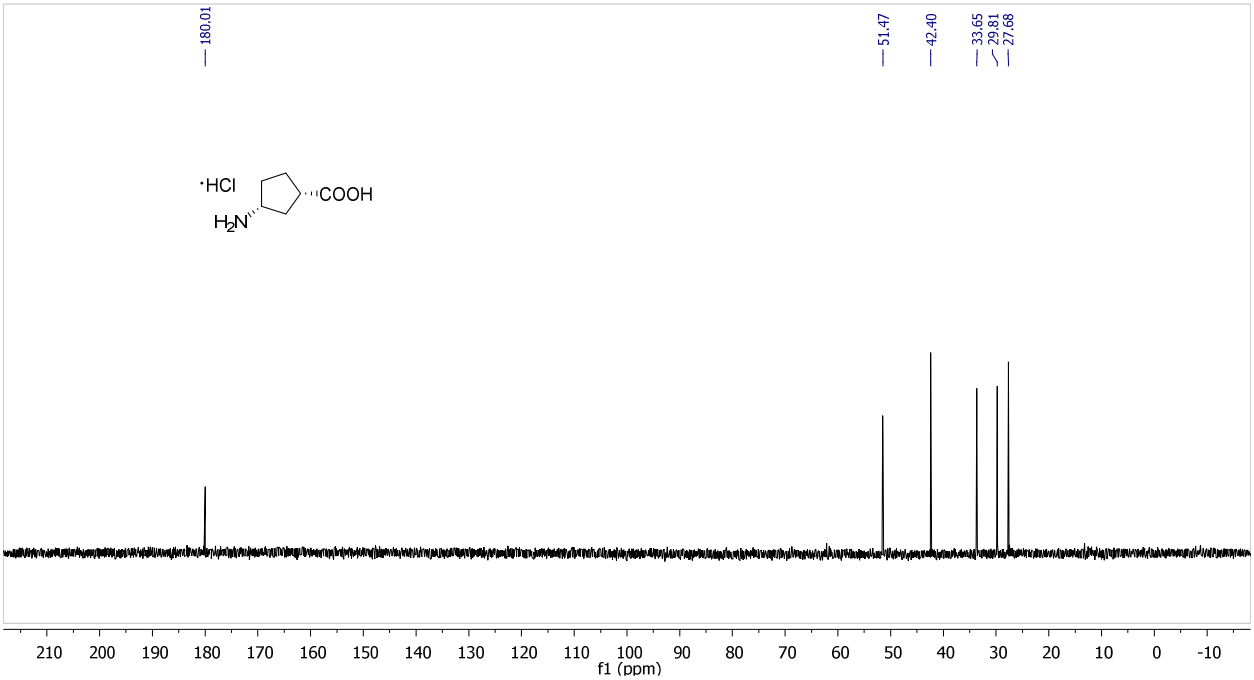


**Figure S24.** [13]C NMR Spectrum of **39**

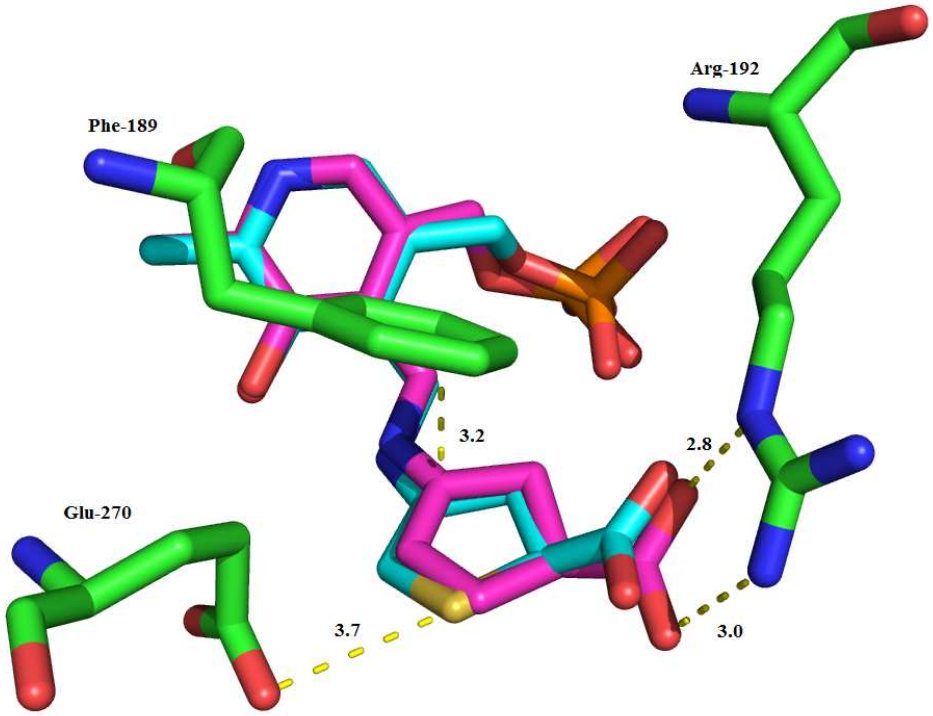


**Figure S25.** Overlay of *in silico* model of compound PLP-**39** adduct (pink) and PLP-**17** adduct (cyan), as well as key nearby residues

The molecular modeling studies of the PLP adduct with **39** were performed using the GOLD software package, version 5.3 (Cambridge Crystallographic Data Center, Cambridge, UK). The X-ray coordinates of adduct **34** bound to GABA-AT were used, and the active site was defined as a sphere enclosing residues within 10 Å around **34**. The 3D structure of **39** was built using ChemBio Ultra (version 14.0) and was energy minimized using an MM2 force field for 1000 iterations and a convergence value of 0.01 kcal/mol/ Å as the termination criterion. The energy minimized PLP-**39** was docked in the binding site of GABA-AT (without **34**) and scored using ChemPLP fitness function. All poses generated by the program were visualized; however, the pose with the highest fitness score was used for elucidating the binding characteristics of **39** in the GABA-AT active site. Pymol (version 1.1) was used for generating the image in Figure S25.